Transaction B: Mechanical Engineering
Vol. 17, No. 3, pp. 217–228

Research Note

SCIENTIA IRANICA

Robust Control of Non-linear Flexible Spacecraft

M. Malekzadeh[1,*], A. Naghash[1] and H.A. Talebi[2]

Abstract. *In this paper, the problem of attitude control of a 1D non-linear flexible spacecraft is investigated. Three controllers are presented. The first is a non-linear dynamic inversion, the second is a linear μ-synthesis and the third is a composition of dynamic inversion and a μ-synthesis controller. It is assumed only one reaction wheel is used. Actuator saturation is considered in the design of controllers. The performances of the proposed controllers are compared in terms of nominal performance, robustness to uncertainties, vibration suppression of panels, sensitivity to measurement noise, environment disturbance and non-linearity in large maneuvers. To evaluate the performance of the proposed controllers, an extensive number of simulations on a non-linear model of the spacecraft are performed. Simulation results show the ability of the proposed controller in tracking the attitude trajectory and damping panel vibration. It is also verified that the perturbations, environment disturbance and measurement errors have only slight effects on the tracking and damping responses.*

Keywords: *Non-linear flexible spacecraft; Dynamic inversion; μ-synthesis; Actuator saturation.*

INTRODUCTION

Modern spacecraft often employ large flexible structures such as solar arrays to provide sustainable energy during space flight. When it is required to maneuver the attitude of the flexible spacecraft, the dynamic coupling between the solar panel vibration and the spacecraft attitude varies with the angle of attitude maneuver. The equations that govern attitude maneuvers and attitude tracking are non-linear and coupled, thus, the attitude control system must consider these non-linear dynamics.

A common method to control space vehicles is to use a linear controller calculated for the linear approximation of the non-linear system around an operating point. This method is largely used due to the fact that, for linear systems, there are plenty of well established control techniques, and the design can be done in a more systematic way than in the non-linear case. Nevertheless, this kind of control technique works, in general, only in a small neighborhood of the operating point where the linear approximation is valid. Thus, when the system is far from this point, the linear controller will not behave as desired.

In the context of non-linear systems, the feedback linearization seems to be a viable choice since the non-linear system is exactly transformed into a linear system (valid for the entire operating region) and only then is the linear controller applied. Therefore, the dynamic range of the closed-loop system is increased. However, the classical feedback linearization suffers from the lack of robustness in the presence of uncertainties, disturbances and noise.

In [1], the problem of attitude recovery of flexible spacecraft with plate type appendages using the feedback linearization approach is investigated. The controller ability is shown in the recovery maneuver and panel vibration suppression. However, the performance is only tested for impulse disturbance (thruster effect)- it is notable that feedback linearization is robust against impulse disturbance but is very weak against constant disturbances. Although this method achieves good vibration suppression, it does not address the issue of robustness to combined uncertain conditions (several uncertain conditions, i.e. environment disturbance, sensor noise and uncertain parameters exist together, or one uncertain condition with larger

1. *Department of Aerospace Engineering, Amirkabir University of Technology, Tehran, P.O. Box 15875-4413, Iran.*
2. *Department of Electrical Engineering, Amirkabir University of Technology, Tehran, P.O. Box 15875-4413, Iran.*
*. *Corresponding author. E-mail: malekzadeh@aut.ac.ir*

Received 24 January 2009; received in revised form 2 December 2009; accepted 4 April 2010

variations). Moreover, the selected controller bound is large as if actuator saturation has not been considered.

Recently, considerable efforts have been made to design robust control systems for simultaneous attitude control and vibration suppression of flexible spacecraft. However, most of them are based on a linear control approach, which results in a poor performance for large maneuvers. For instance, in [2], an experimental flexible arm serves as a test bed to investigate the efficiency of the μ-synthesis design technique in controlling flexible manipulators. In [3], the active optimal attitude control of a three-axis stabilized spacecraft by flywheels is studied. The corresponding time-varying Linear Quadratic Regulators (LQR) are designed for an approximate system.

Recent papers have discussed non-linear robust methodologies for the control of flexible mechanical systems. In [4], a sliding mode control strategy for a three-axis attitude maneuver of a flexible spacecraft model is proposed. However, the issue of panel vibration has not been addressed. In [5], a new approach is presented for vibration reduction of flexible spacecraft during attitude maneuvers by using the variable structure control theory to design switching logic for thruster firing. Lead Zirconate Titanate (PZT) is used as a sensor and actuator for active vibration suppression; hence, the resulting controller is not collocated.

Although non-linear robust control methods, such as non-linear H_∞ control, can be applied to address these issues, solving the associated Hamilton-Jacobi equation is often extremely complicated, and the resulting controller is not easy to implement. Consequently, a robust feedback linearization strategy seems promising.

In [6], an adaptive feedback linearizing control law is derived for the trajectory control of the pitch angle. Unmodeled parameters appearing in the inverse feedback linearization control law are estimated using a high gain observer. However, other uncertainties, such as sensor noise and environment disturbances, have not been considered. In [7], a hybrid control scheme with a variable structure and an intelligent adaptive control method are used for the control of flexible space structures.

The objective of this paper is proposing a new approach for the robust attitude control and vibration suppression of flexible spacecraft. A μ-synthesis control law is formulated such that an outer-loop linear controller can be constructed to provide a robust stability/performance against the inexact dynamic cancellation arising in the inner-loop feedback linearization design. It is notable that the proposed composite controller has not yet been applied to spacecraft.

In this paper, the attitude control of a 1D flexible spacecraft is considered using three approaches: dynamic inversion, μ-synthesis and a composition of dynamic inversion and μ-synthesis. The goal is attitude control and panel vibration suppression in the absence of damping and actuators on panels.

In the design of a dynamic inversion controller, attitude angles are considered as the output, and panel deflection is used for feedback. To enforce the position and rate saturation limit, a feedback controller structure is used in the inner loop. The internal dynamic and closed-loop stability is shown using the Lyapunov method. In the design of a μ-synthesis controller, attitude angles and panel deflection are considered as the output. Moreover, in the design of a composed controller, it is often the case that the linearized model is different from the linear model. Hence, choosing weighting functions is very challenging. Another important issue in designing the μ-synthesis controller is bounding the linear controller term, which is different from the bound for the actual control signal, u. Hence, it is crucial to find an appropriate weighting function for the linear controller. To evaluate the performance of the proposed controllers, a set of simulations are performed on a one-dimensional stabilized flexible spacecraft. It was our intention that the sensors noises, disturbances and uncertainty be as close as possible to practical situations.

The paper is organized as follows: In the next section, dynamic equations of flexible spacecraft are considered. The design of three controllers, namely, nonlinear dynamic inversion, linear robust (μ-synthesis method) and inner loop feedback linearization and outer loop μ-synthesis controllers will be presented in the following sections, respectively. Following that, the computer simulations of attitude tracking and panel vibration suppression for these controllers are included. Finally, some conclusions will be drawn.

FLEXIBLE SPACECRAFT DYNAMIC

The system under investigation consists of a rigid hub and 2 appendages attached to it. According to Figure 1, each appendage has linear density (mass per unit length) ρ, length l, and is attached at distance r from the hub.

The kinetic energy of the system is composed of kinetic energies of the hub, and the appendages. This

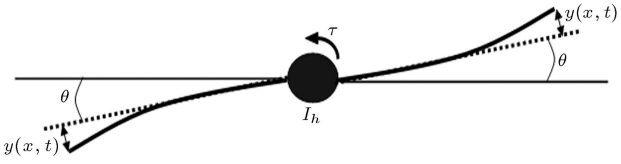

Figure 1. Flexible spacecraft model.

kinetic energy can be written in the form of:

$$T = \frac{1}{2}J_h\dot{\theta}^2 + \int \rho[(r+x)^2\dot{\theta}^2 + 2(r+x)\dot{\theta}\dot{y} + \dot{y}^2 + y^2\dot{\theta}^2]dx. \quad (1)$$

The potential energy does not include a gravity term and is just the usual potential energy of the beam bending deformation of the form:

$$V = \int EIy''^2 dx. \quad (2)$$

To derive the dynamic model of the described system, the assumed modes formulation of the flexible appendage dynamics is used. Flexible deflection of the appendages along the body axis is of the form:

$$y = \sum_{i=1}^{N} \varphi_i q_i, \quad (3)$$

where q_i are modal coordinates, N is the number of the assumed modes considered, and φ_i are shape functions of the appendage deformation. The following shape function is an acceptable candidate for a clamped beam [8].

$$\varphi_i = 1 - \cos\left(\frac{i\pi x}{l}\right) + \frac{1}{2}(-1)^{i+1}\left(\frac{i\pi x}{l}\right)^2. \quad (4)$$

The vibration equations of motion are obtained by using the conventional form of the Lagrange equation.

$$\frac{d}{dt}\left(\frac{\partial L}{\partial \dot{\theta}}\right) - \frac{\partial L}{\partial \theta} = \tau,$$

$$\frac{d}{dt}\left(\frac{\partial L}{\partial \dot{q}}\right) - \frac{\partial L}{q} + \frac{\partial}{\partial q}\left(\frac{\partial L}{\partial q'}\right) - \frac{\partial^2}{\partial q^2}\left(\frac{\partial L}{\partial q''}\right) = 0,$$

where $L = T - V$.

Substituting the kinetic and potential energy equations in the Lagrange equation, the final form of the vibration equation is obtained:

$$J_h\ddot{\theta} + 2\int \rho(r+x)^2 dx\ddot{\theta} + \int \rho\varphi_i q_i \sum \varphi_i q_i \ddot{\theta} + 2\int \rho(r+x)\sum \varphi_i \ddot{q}_l + 2\int \rho\varphi_i q_i^T \sum \varphi_i q_i \dot{\theta} = \tau, \quad (5)$$

$$2\int \rho(r+x)\sum \varphi_i dx\ddot{\theta} + 2\int \rho\varphi_i \sum \varphi_i \ddot{q}_l + 2\int EI\varphi_i'' \sum \varphi_i'' \ddot{q}_l = 0. \quad (6)$$

The above equation may be rewritten in a simple form:

$$\begin{bmatrix} J + q^T M_{qq} q & M_{\theta q} \\ M_{\theta q} & M_{qq} \end{bmatrix}\begin{bmatrix}\ddot{\theta}\\ \ddot{q}\end{bmatrix} + \begin{bmatrix} 0 & 0 \\ 0 & K_{qq} - \dot{\theta}^2 M_{qq}\end{bmatrix}\begin{bmatrix}\theta\\ q\end{bmatrix} + \begin{bmatrix} 2 & q^T M_{qq} & q\dot{\theta} \\ & 0 & \end{bmatrix} = \begin{bmatrix}\tau\\ 0\end{bmatrix}. \quad (7)$$

The modal cross-inertia vector, $M_{\theta q}$, modal inertia matrix, M_{qq}, and modal stiffness matrix, K_{qq}, are defined through the shape functions.

With regard to a small q, by neglecting the high order term of q, this equation can be linearized as:

$$\begin{bmatrix} J & M_{\theta q} \\ M_{\theta q} & M_{qq}\end{bmatrix}\begin{bmatrix}\ddot{\theta}\\ \ddot{q}\end{bmatrix} + \begin{bmatrix} 0 & 0 \\ 0 & K_{qq}\end{bmatrix}\begin{bmatrix}\theta\\ q\end{bmatrix} = \begin{bmatrix}\tau\\ 0\end{bmatrix}. \quad (8)$$

To include structural damping, a proportional damping term is added to Equation 6 which results in a diagonal damping matrix, D, with entries γ_1 and γ_2 as damping parameters [8].

$$D = \gamma_1 M_{qq} = \gamma_2 K_{qq}, \quad (9)$$

$$M_{\theta q}\ddot{\theta} + M_{qq}\ddot{q} + D\dot{q} + (K_{qq} - \dot{\theta}^2 M_{qq})q = 0. \quad (10)$$

FEEDBACK LINEARIZATION

It is assumed that no actuators are available on the flexible beam-type appendages, hence, exact feedback linearization (i.e. input-state) cannot be performed and we must turn to the input-output feedback linearization (or so called dynamic inversion [9]) control technique (Figure 2).

It is assumed that a full state measurement of the system is available through attitude (e.g. sun sensors, gyros and accelerometers). Consider the dynamic equations of attitude of a flexible spacecraft; assuming 1 panel and 1 mode:

$$(J = q^T M_{qq} q)\ddot{\theta} + M_{\theta q}\ddot{q} + 2\dot{\theta}q^T M_{qq} q = \tau, \quad (11\text{-}1)$$

$$M_{\theta q}\ddot{\theta} + M_{qq}\ddot{q} + D\dot{q} + (K_{qq} - \dot{\theta}^2 M_{qq})q = 0. \quad (11\text{-}2)$$

The repeated differentiation process is done on the

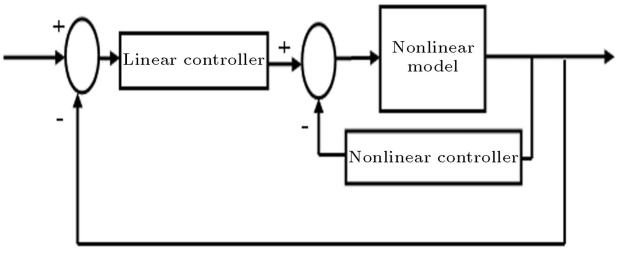

Figure 2. Feedback linearization method.

output (attitude angle) until the control signal appears:

$$\vec{Y} = \vec{\theta} \xrightarrow{\text{yields}} \dot{\vec{Y}} = \dot{\vec{\theta}} = \vec{\omega} = \nu. \tag{12}$$

By calculating $\ddot{q}$ from Equation 11-2 and putting it in Equation 11-1 the following will be obtained:

$$\ddot{q}^* = -M_{qq}^{-1}\{M_{\theta q}\ddot{\theta} + (K_{qq} - \dot{\theta}^2 M_{qq})q\}, \tag{13}$$

$$\tau = (J + q^T M_{qq} q)\ddot{\theta} + M_{\theta q}\ddot{q}^* + 2\dot{\theta} q^T M_{qq} q. \tag{14}$$

According to the following equation:

$$\tau = I(q)\nu - M_{\theta q}M_{qq}^{-1}\{M_{\theta q}\nu + (K_{qq} - \dot{\theta}^2 M_{qq})q\} + 2\dot{\theta} q^T M_{qq} q, \tag{15}$$

where $I(q) = J + q^T M_{qq} q$.

The coefficient, $I(q)$, in the specific case ($q = 0$) is equal to J and in other cases it can also be shown that this term is invertible. Hence, the signal, ν, should be constructed to control the new linear system. The system can be controlled by introducing a linear controller of the form:

$$\nu = \omega_\theta^2 \theta_e - 2\xi_\theta \omega_\theta \dot{\theta} + \omega_n^2 q_e - 2\xi_q \omega_q \dot{q}. \tag{16}$$

The flexible spacecraft with one panel, and considering one elastic mode, has the order of 4. By considering the output as $y = \theta$ and differentiating the output of the system 2 times to generate an explicit relationship between output y and controller input τ, it is clear that the relative degree is $r = 2 < n = 4$.

Therefore, parts of the system dynamics have been rendered 'unobservable' in the input-output linearization. This part of the dynamics will be called internal dynamics, because it cannot be seen from the external input-output relationship.

To keep the notation simple, a linear system in state space form is considered:

$$\dot{x} = f(x) + g(x)\tau.$$

The new set of states can be defined by:

$$X = \begin{bmatrix}\theta & \dot{\theta} & q & \dot{q}\end{bmatrix}.$$

Choosing the state vector as X, The corresponding vector fields, f and g, can be written as:

$$f(x) = \begin{bmatrix} \dot{\theta} \\ A_{\theta q}(M_{\theta q}M_{qq}^{-1}(K_{qq} - \dot{\theta}^2 M_{qq})q - 2\dot{\theta} q^T M_{qq} q) \\ \dot{q} \\ -M_{qq}^{-1}(M_{\theta q}A_{\theta q}((M_{\theta q}M_{qq}^{-1} + 1) \\ \quad (K_{qq} - \dot{\theta}^2 M_{qq})q + D\dot{q} - 2\dot{\theta} q^T M_{qq} q)) \end{bmatrix}, \tag{17}$$

$$g(x) = \begin{bmatrix}0 & A_{\theta q} & 0 & -M_{qq}^{-1}M_{\theta q}A_{\theta q}\end{bmatrix}, \tag{18}$$

$$A_{\theta_q} = (J + q^T M_{qq} q - M_{\theta q}M_{qq}^{-1}M_{\theta q})^{-1}. \tag{19}$$

In order to find the normal form, take $\mu_1 = \theta$ and $\mu_2 = \dot{\theta}$. From Equation 19, we can write:

$$\dot{\mu}_1 = \mu_2,$$

$$\dot{\mu}_2 = A_{\theta q}(M_{\theta q}M_{qq}^{-1}(K_{qq} - \dot{\theta}^2 M_{qq})q - 2\dot{\theta} q^T M_{qq} q) + A_{\theta q}\tau, \tag{20}$$

The third function $\psi(x)$ is required to complete the transformation, which brings the dynamics to their normal form. It should satisfy the following equation:

$$L_{g_j}\psi_k = \frac{\partial \psi_k}{\partial x} g_j = 0,$$

$$\frac{\partial \psi_i}{\partial \dot{\theta}} A_{\theta q} + \frac{\partial \psi_i}{\partial \dot{q}}(-M_{qq}^{-1}M_{\theta q}A_{\theta q}) = 0. \tag{21}$$

One solution of this equation is:

$$\psi_1 = q, \qquad \psi_2 = M_{qq}^{-1}M_{\theta q}\dot{\theta} + \dot{q}. \tag{22}$$

By differentiating these functions and by using system dynamics, the internal dynamics are obtained as:

$$\dot{\psi}_1 = \dot{q},$$

$$\dot{\psi}_2 = M_{qq}^{-1}(K_{qq} - \mu_2^2 M_{qq})\psi_1 - M_{qq}^{-1}d\dot{q}, \tag{23}$$

$$\dot{\psi} = \begin{bmatrix}\dot{\psi}_1 \\ \dot{\psi}_2\end{bmatrix} = \begin{bmatrix} \psi_2 - M_{qq}^{-1}M_{\theta q}\mu_2 \\ M_{qq}^{-1}(K_{qq} - \mu_2^2 M_{qq}\psi_1 \\ \quad - M_{qq}^{-1}D(\psi_2 - M_{qq}^{-1}M_{\theta q}\mu_2) \end{bmatrix}. \tag{24}$$

It is shown that the local asymptotic stability of zero-dynamics is enough to guarantee the local asymptotic stability of the internal dynamics. Zero dynamics are defined to be the internal dynamics of the system when the system output is kept at zero by the input.

$$\dot{\psi}(0, \psi) = w(0, \psi), \tag{25}$$

$$\dot{\psi}_1 = \psi_2, \tag{26-1}$$

$$\dot{\psi}_2 = -M_{qq}^{-1}K_{qq}\psi_1 - M_{qq}^{-1}D\psi_2 \tag{26-2}$$

By differentiating Equation 26-2 and substituting Equation 26-1, the zero dynamics can be written as:

$$\ddot{\psi}_2 + M_{qq}^{-1}D\dot{\psi}_2 + M_{qq}^{-1}K_{qq}\psi_2 = 0. \tag{27}$$

Since γ_1, γ_2 and $K_{qq} > 0$, we can conclude that zero dynamics are asymptotically stable.

In most modern spacecraft, momentum exchange devices are used as actuators. Due to the saturation effect in these actuators, considering saturation is very important. It has been shown by several authors

that enforcing actuator constraints for input-output linearization can result in a poor closed-loop performance (when compared to an unconstrained closed loop performance) [10]. Different methods have been successfully demonstrated that assist in preventing the destabilizing effects of control saturations in the feedback linearization method. In most cases, saturation is considered by designing a special outer loop (linear) controller; hence, these methods cannot be used in this paper. To enforce the position and rate of the saturation limits, feedback controller structures are used [10-12]. Most of these structures filter the peak of the response. Simulation studies show that considering saturation in inner and outer loops together is more effective. In this paper, the structure shown in Figure 3 is used [11]. The gain can be chosen depending on the bounds of the output response. In appropriate scaling, tanh can be used to represent saturation behavior:

$$u_{\text{sat}} = \tan\ \text{h}\left(\frac{u}{u_{\max}}\right) u_{\max}. \tag{28}$$

By defining the following parameters:

$$A_{\theta q} = J + q^T M_{qq} q - M_{\theta q} M_{qq}^{-1} M_{\theta q}, \tag{29}$$

$$A_{dd} = M_{\theta q} M_{qq}^{-1} (K_{qq} - \dot{\theta}^2 M_{qq}) q - 2\dot{\theta} q^T M_{qq} q. \tag{30}$$

Equation 15 can be written as:

$$A_{\theta q} \ddot{\theta} = A_{dd} + \tau. \tag{31}$$

Let δ be the difference between the calculated controller and the applied control:

$$\delta = u_c - u_a. \tag{32}$$

From Equations 31 and 32:

$$A_{\theta q} \ddot{\theta} = A_{dd} + \tau + \delta. \tag{33}$$

The linearized model takes the following form:

$$\ddot{\theta} = \nu + A_{\theta q}^{-1} \delta. \tag{34}$$

As shown in Equation 34, the hedge signal, $A_{\theta q}^{-1}\delta$, acts as a disturbance.

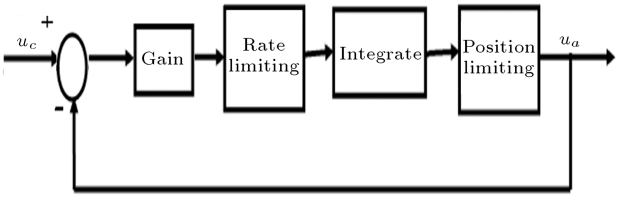

Figure 3. Enforcing Control saturation limits.

μ-SYNTHESIS CONTROLLER

Equation 8 is the linear equation of motion for flexible spacecraft. The advantage of the μ-synthesis approach is that it allows the direct inclusion of modeling errors or uncertainties, measurement and control inaccuracies, and performance requirements into a common control problem formulation. These uncertainties include: unmodeled high frequency dynamics, errors in natural frequencies and damping levels, and actuator and sensors errors.

According to low and high frequency uncertainties in a flexible spacecraft model, two uncertainties are included in the control problem formulation. A multiplicative input uncertainty model, W_Δ, accounts for actuator errors in high frequencies, and unmodeled actuator dynamics and the additive uncertainty, denoted by W_{additive}, account for high-frequency dynamics and non-linearities neglected in the design model.

To choose low frequency weight, W_Δ, different system parameters (such as J, $M_{\theta q}$, M_{qq} and K_{qq}) were perturbed by 20% of their nominal values. The nominal transfer function $\left(\frac{\theta}{\tau}\right)$ of the system was selected. Then, the bode diagram of the actual system and the nominal transfer function plus the multiplicative weighting functions were obtained. The weighting functions were then tuned to get the best possible match which is obtained for:

$$W_\Delta = \frac{3(s+1)}{s+10}. \tag{35}$$

The effect of uncertain parameters on this transfer function and uncertain plant $G(I + W_\Delta \Delta_G)$ is shown in Figure 4.

W_{additive} is added to the panel vibration deflection. To include the uncertainty in the model, different system parameters were perturbed by 20% of their nominal values. Then, the bode diagram of the actual

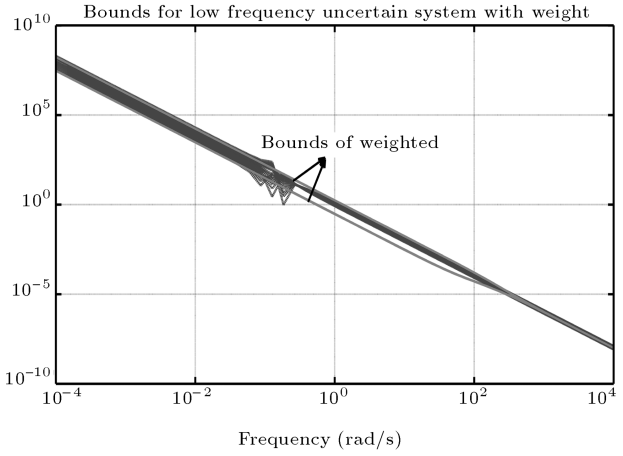

Figure 4. Bounded of low frequency uncertainties and weight.

system, $\frac{y}{\tau}$, and the nominal transfer function plus the additive weighting functions were obtained. The weighting functions were then tuned to get the best possible match which is obtained for:

$$W_A = \frac{0.3(0.631s^2 + 5.31s + 22.62)}{s^2 + 59.41s + 2270}. \quad (36)$$

The effect of uncertain parameters on the transfer function and uncertain plant, $G + W_A\Delta$, is shown in Figure 5.

The additive uncertainty level is of less importance when the models of the higher frequency modes are available to the designer.

A feedback system with the following block diagram can be rearranged as a lower Linear Fractional Transformation (LFT). The controller structure is shown in Figure 6.

A concern is that as the number of states in the problem formulation increases the accuracy of the numerical solution decreases. This provides a reason to limit the states in the problem formulation. So, in this paper, the controller is designed using pitch angle and tip displacement feedback. A performance tip weight

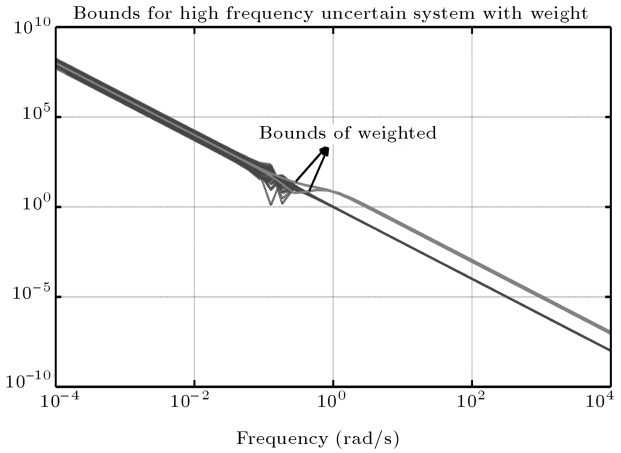

Figure 5. Bounded of high frequency uncertainties and weight.

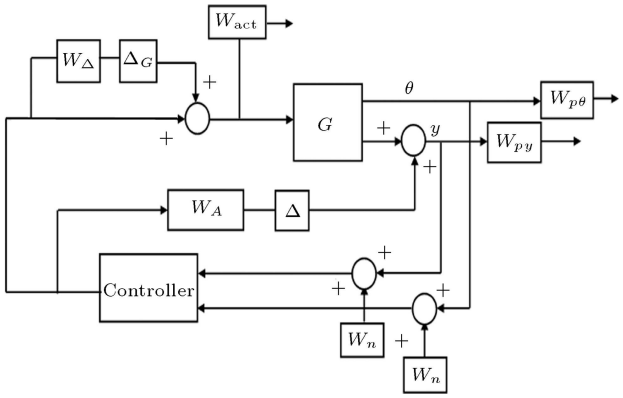

Figure 6. μ-synthesis arrangement block diagram.

of constant magnitude equal to 0.1 is applied to the system.

The hub performance weighting function is chosen by considering the desired transient performance measures, such as settling time and overshoot:

$$W_{p\theta} = \frac{0.98(s^2 + s + 0.25)}{(s^2 + 4s + 0.9)}. \quad (37)$$

W_{act} is the actuator saturation limitation weighting function. It may be used to reflect the restrictions on the control or actuator signals. To achieve a robust performance, it is necessary that $||W_{\text{act}}\tau|| < 1$, so, $W_{\text{act}} < \frac{1}{\tau}$. According to the actuator saturation limitation, $|\tau| < 0.8$ N.m, W_{act} is set to $W_{\text{act}} = 1$.

The weighting function, W_n, is used to model sensor noise associated with the hub-angle and tip-displacement sensors corresponding to the measurement noise. It is assumed that the angular velocity and the pitch angle are measured by the rate gyro and earth sensor corrupted with a random measurement noise of magnitude 0.1 deg per second and 0.2 deg. The velocity and acceleration of the point on the flexible panel is measured by a tachometer and accelerometers with a random measurement noise of 0.0001 m/s and 0.0001 m/s^2. W_n is a high-pass filter, according to the nature of the high frequency noise. Hence, we have:

$$W_{n\theta} = \left(\frac{0.2\pi}{180}\right)\frac{0.12s + 1}{0.001s + 1},$$

$$W_{nq} = (3 \times 10^{-4})\frac{0.12s + 1}{0.001s + 1}. \quad (38)$$

The resulting controller is stable and of high order. This is obviously not practical and it should be reduced without significant performance degradation. Using balanced truncation, the order of the controller is reduced to 7 without much loss of the closed-loop performance or robustness.

DESIGN OF COMPOSITE CONTROLLER

The performance of feedback linearization is rather poor in the presence of uncertainty, disturbance and noise. Due to the uncertainty, inexact dynamic cancellation arises in the inner-loop feedback linearization design. Hence, a μ-synthesis control law is added as an outer-loop linear controller. Dynamic inversion and structured singular value synthesis are combined to achieve robust control of flexible spacecraft. The controller structure is shown in Figure 2. In this method, non-linear dynamics are linearized by an input-output feedback linearization method. The new linear system is in the form of $\ddot{\theta} = \nu$, so, a new control signal, ν, should be designed.

The advantage of the μ-synthesis method is that it allows the direct inclusion of modeling errors or

uncertainties, measurement and control inaccuracies, and performance requirements into a common control problem formulation.

By considering uncertainty on parameters such as J, M_{qq}, $M_{\theta q}$ and K_{qq}, Equation 31 can be written as:

$$A_{\theta q}\ddot{\theta} - A_{dd} = \hat{A}_{\theta q}\nu - \hat{A}_{dd}, \tag{39}$$

where:

$$\Delta A_{\theta q} = A_{\theta q} - \hat{A}_{\theta q},$$

and:

$$\Delta A_{dd} = A_{dd} - \hat{A}_{dd},$$

denote the parametric uncertainty.

$$\ddot{\theta} = A_{\theta q}^{-1}\hat{A}_{\theta q}\nu + A_{\theta q}^{-1}(A_{dd} - \hat{A}_{dd}). \tag{40}$$

By substituting real parameters, Equation 40 can be written as:

$$\begin{aligned}\ddot{\theta} &= A_{\theta q}^{-1}(A_{\theta q} - \Delta A_{\theta q})\nu + A_{\theta a}^{-1}(A_{dd} - \hat{A}_{dd}) \\ &= \nu - A_{\theta q}^{-1}\Delta A_{\theta q}\nu + A_{\theta q}^{-1}\Delta A_{dd}.\end{aligned} \tag{41}$$

As Equation 41 shows, uncertain parameters result in a multiplicative uncertainty in controller input ($A_{\theta q}^{-1}\Delta A_{\theta q}$), and a disturbance, $A_{\theta q}^{-1}\Delta A_{dd}$. The controller structure is shown in Figure 7.

To include the uncertainty in the model, different system parameters (such as J, M_{qq}, $M_{\theta q}$, K_{qq}) were perturbed by 20% of their nominal values. Then, the nominal transfer function $\left(\frac{1}{s^2}\right)$ of the system was selected as a double integrator, i.e. $\frac{1}{s^2}$. The bode diagram of the actual system, and the nominal transfer function plus the multiplicative weighting functions were obtained. The weighting functions were then tuned to get the best possible match which is obtained for:

$$W_\Delta = \frac{70(s+1)}{s+100}. \tag{42}$$

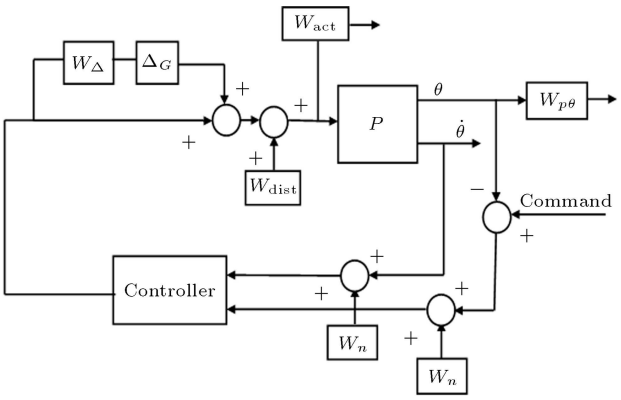

Figure 7. Composite arrangement block diagram.

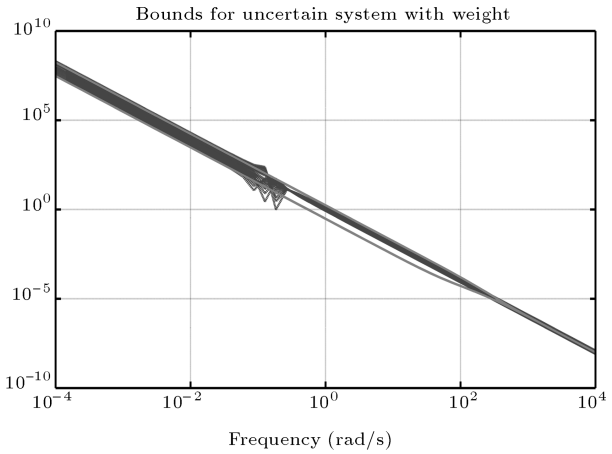

Figure 8. Bounded of uncertainties and chosen weight.

The effect of uncertain parameters on the transfer function and uncertain plant $P(I + W_{\Delta_G}\Delta)$ is shown in Figure 8. This uncertainty description must be sufficiently large to require the control design to stabilize unmodeled modes.

W_p weights the error between the complementary sensitivity function of the closed loop system and an ideal model of the system response. The performance objective can be written as $|W_p S| \leq 1$. So, W_p should be selected such as $W_P < \frac{1}{||S||}$. According to the first and third frequency of the vibration modes of a flexible panel, this function is chosen as:

$$W_{p\theta} = \frac{0.1(s^2 + s + 0.25)}{(s^2 + 4s + 0.01)}. \tag{43}$$

Therefore, the hub performance weight has a relatively large magnitude at low frequencies.

According to the weakness of the dynamic inversion method against constant disturbance, a disturbance weight is chosen, such as:

$$\frac{W_{\text{dist}}}{|\nu|} = \frac{W_{\text{distact}}}{|\tau|}. \tag{44}$$

W_{distact} of constant magnitude equal to 0.001 is applied to the system. The parametric uncertainty disturbance in Equation 41 is very small, so, in comparison, it has not been considered.

To enforce the controller saturation limits in the inner loop, the feedback controller structure shown in Figure 3 is used. Also, this saturation can be considered in the designing of a μ-synthesis controller; however, using the dynamic inversion formulation, the actuator dynamics are not directly accessible. In [10], an algorithm is derived to catch the bound on ν in the feedback linearization outer loop, according to the actuator saturation limit. In this paper, this limit is approximately obtained, according to the following

equation, by assuming a small q:

$$\tau = (J + q^T M_{qq} q)\nu - M_{\theta q} M_{qq}^{-1}\{M_{\theta q}\nu + (K_{qq} - \dot{\theta}^2 M_{qq})q\} + 2\dot{\theta} q^T M_{qq} q. \quad (45)$$

According to the actuator saturation limitation:

$$W_{\text{act}} = 500. \quad (46)$$

The new input torque, ν, is obtained by adding two terms, $\zeta\omega_n\dot{q}$ and $\omega_n^2 q$. These terms are added to the μ-synthesis controller output to increase the rate of vibration suppression of the appendages. Without these terms, the time constant of vibration suppression is too high and not optimal for practical implementation. The gain parameters are chosen as $\omega_n = 0.2$ and $\zeta = 1$.

SIMULATIONS AND RESULTS

In this section, simulation results for the closed loop system (Equation 12), with the control laws derived in the previous sections, are presented using MATLAB and SIMULINK software. In the simulation, the system parameters are chosen the same as those in [1]. $EI = 1500$ N/m^2, $\rho = 0.2$ kg/m, $l = 30$ m, $J_n = 4000$ kgm^2, $r = 1$ m.

The control input and its rate are bounded as:

$$|u| < 0.8 \quad \text{N.m}, \qquad |\dot{u}| < 0.8 \quad \text{N.m/s}. \quad (47)$$

The environmental disturbances (i.e. gravity gradient, solar pressure, aerodynamic and magnetic torques) on the spacecraft are obtained from the following equation:

$$\tau_d = 0.005 - 0.05\sin\left(\frac{2\pi t}{400}\right) + \delta(200, 0.2) + \nu_1, \quad (48)$$

where $\delta(T, \Delta T)$ denotes an impulsive disturbance with magnitude 1, period T, and width ΔT. The terms ν_1 denote white Gaussian noise with mean values of 0 and variances of 0.005^2.

It is assumed that angular velocity and pitch angle are measured by the rate gyro and the earth sensor, respectively, which are corrupted with random measurement noise. Earth sensor noise has Gaussian distribution, zero mean and a standard deviation of 0.2 degrees. The Gyro noise sources correspond to a random drift rate and a random bias rate. This model is represented by the following Laplace transformed equation:

$$\omega_M = H_{\text{gyro}}\omega + \omega_D + \omega_N. \quad (49)$$

ω_M and ω are the measured and actual spacecraft angular velocity, respectively. Gyro random bias rate, ω_N, and Gyro random drift noise, ω_D, have Gaussian distribution, with zero mean, and standard deviation of 10^{-6} rad/s. The gyro transfer function is:

$$\text{Hgyro} = \frac{4469s + 89.22}{s^3 + 89.22s^2 + 4469s + 89.22}. \quad (50)$$

The velocity and acceleration of a point on the flexible panel are measured by a tachometer and accelerometers with Gaussian distribution noise, zero mean, and a standard deviation of 0.0001 m/s and 0.0001 m/s^2, respectively. The robustness specification is to account for variation on the values of J, M_{qq}, $M_{\theta q}$ and K_{qq} in Equation 12, which would represent the model parameter uncertainties in the system up to 20%.

In this paper, the gain parameters are chosen as:

$$\omega_\theta = 0.015, \qquad \xi_\theta = 1, \qquad \omega_q = -0.07, \qquad \xi_q = 0.1. \quad (51)$$

In this subsection, a comparison of robustness obtained for the non-linear system with the three proposed controllers (1- feedback linearization 2- μ-synthesis 3- combination of feedback linearization and μ-synthesis) is presented.

A number of time and frequency domain analysis procedures are carried out on the resulting designs and their performance is tested. In all simulations, no damping is considered. The results for the classical feedback linearization, robust (μ-synthesis method) and combined controllers are given in Figures 9-11, respectively.

Feedback Linearization Controller

Figure 9 shows the simulation results of the feedback linearization controller. As compared to Figures 9a, 10a and 11a, in normal conditions, or in conditions wherein only one finite uncertain variation (disturbance, noise and uncertainty) exists, this method shows the best response. It means the feedback linearization design leads to smaller settling times, smaller maximum overshoot and a complete suppression of panel deflection. The dynamic inversion controller achieves this decoupling at the cost of larger control deflections (comparing Figures 9c, 10c and 11c).

However, as shown in Figures 9, in a maneuver or in combined uncertain conditions (several uncertain conditions existing together or one uncertain condition

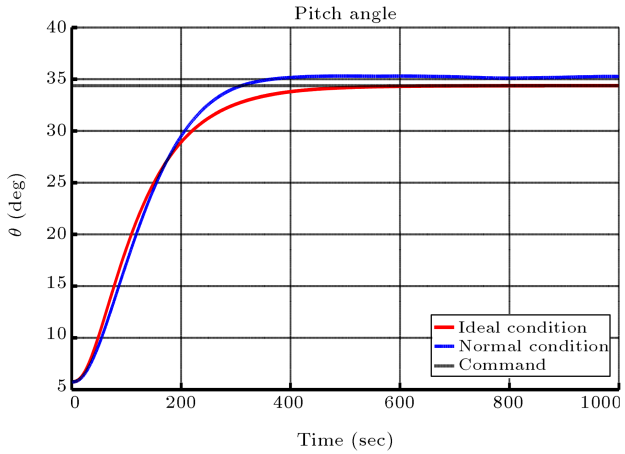

Figure 9a. Spacecraft attitude, dynamic inversion method.

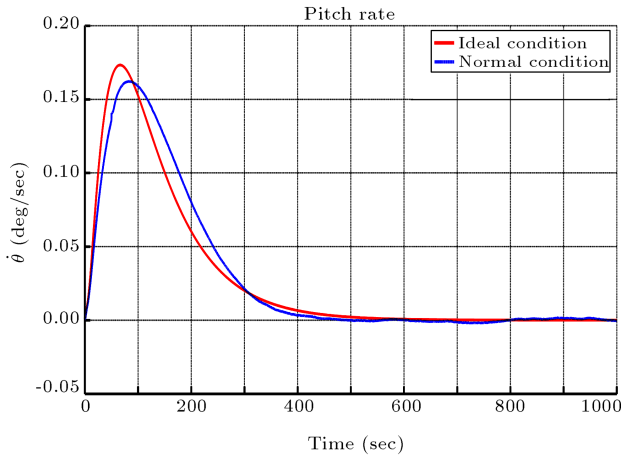

Figure 9b. Body angular velocity, dynamic inversion.

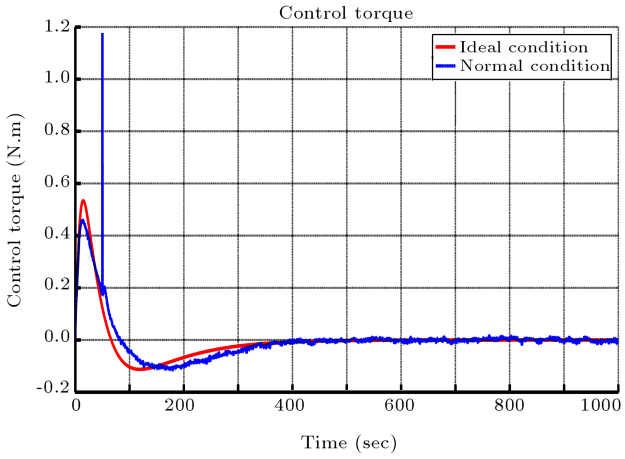

Figure 9c. Reaction wheel torque, dynamic inversion.

with larger variations), much larger control deflections are necessary (out of the maximum acceptable control input) and the attitude rate and position cannot converge completely. In this method, the rate of panel deflection is lower, in comparison with the two other methods.

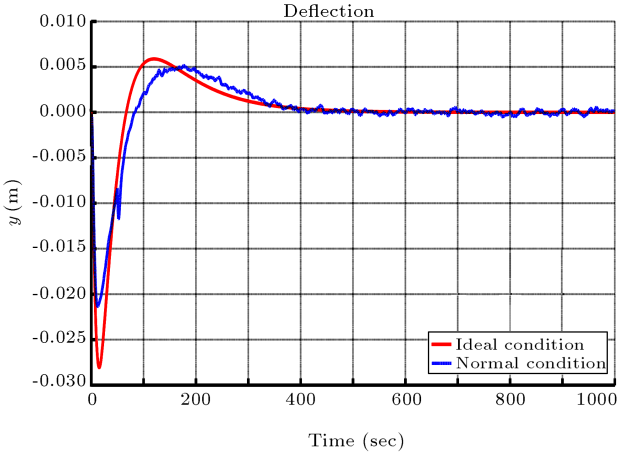

Figure 9d. Tip deflection, dynamic inversion method.

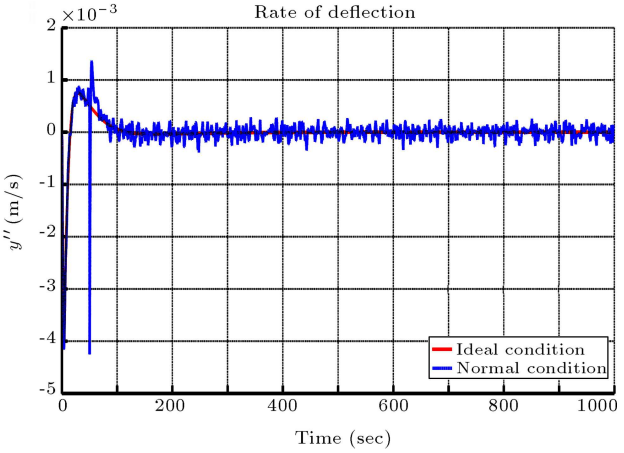

Figure 9e. Rate of tip deflection, dynamic inversion.

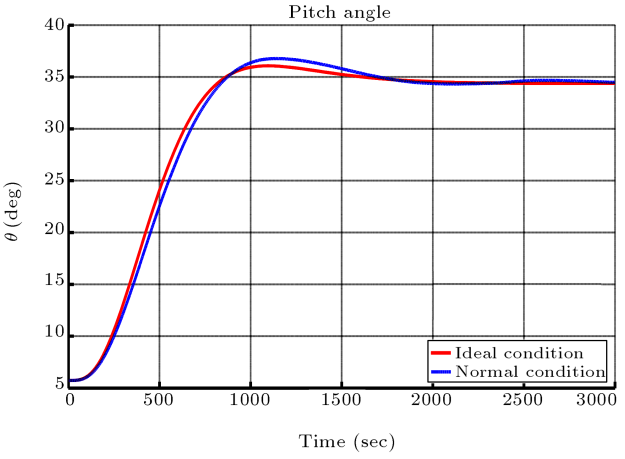

Figure 10a. Spacecraft attitude, μ-synthesis method.

μ-Synthesis Controller

Figure 10 shows the simulation results of the μ-synthesis controller. As shown in Figures 9c and 10c, this procedure requires significantly less iteration effort compared with the feedback linearization case,

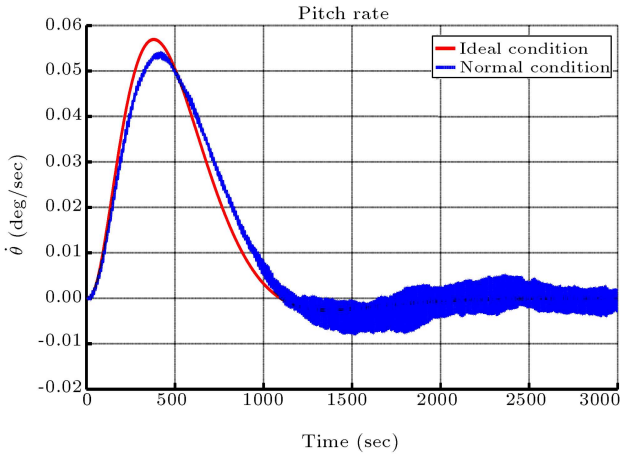

Figure 10b. Body angular velocity, μ-synthesis method.

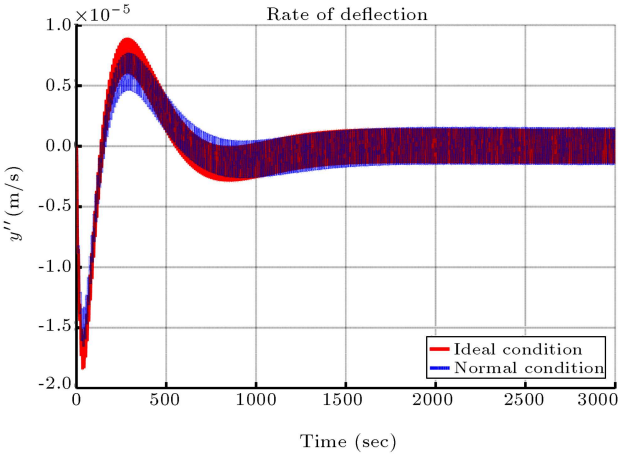

Figure 10e. Rate of tip deflection, μ-synthesis method.

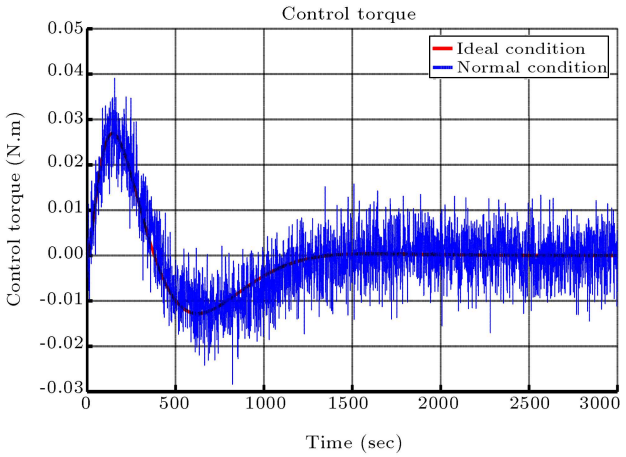

Figure 10c. Reaction wheel torque, μ-synthesis method.

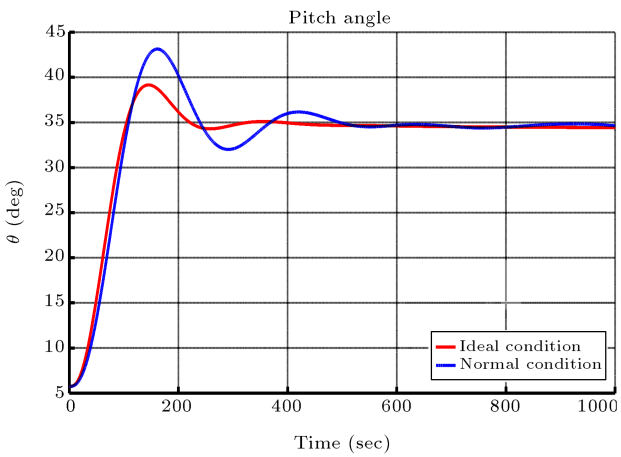

Figure 11a. Spacecraft attitude, composite method.

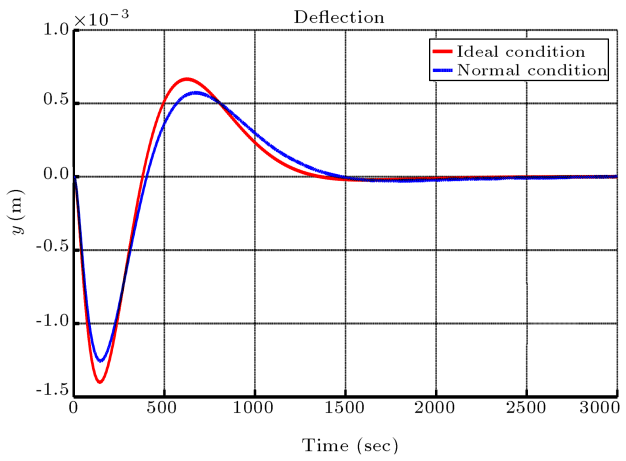

Figure 10d. Tip deflection, μ-synthesis method.

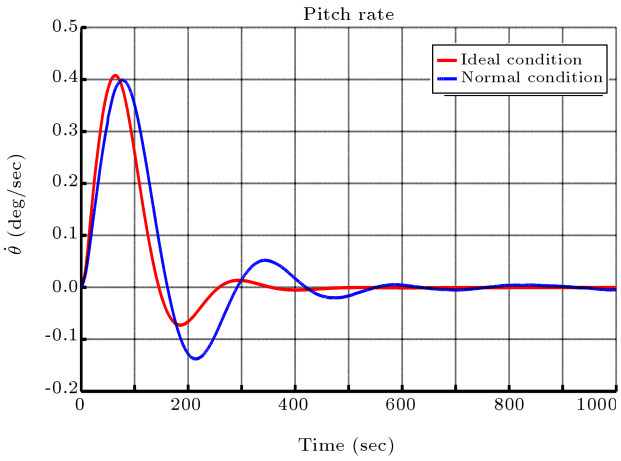

Figure 11b. Body angular velocity, composite method.

to achieve the desired loop shape. As shown in Figure 9, this method performs just as well under combined uncertain conditions (perturbations, disturbance and measurement errors) as under nominal conditions.

The results show that the μ-synthesis method has the longest settling time (compare Figures 9a, 10a, 11a), the highest controller order and less tip deflection (Figures 9d, 10d and 11d).

It is worth mentioning that by increasing uncertainty weight, (W_A and W_Δ), system robustness increased. However, the response has a large overshoot or steady state error (smaller performance) and by

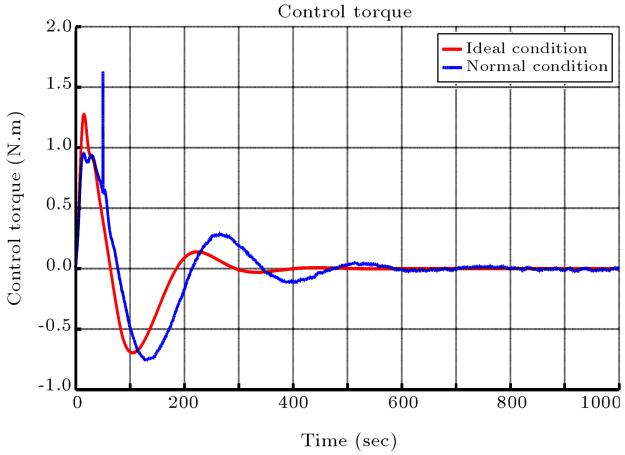

Figure 11c. Reaction wheel torque, composite method.

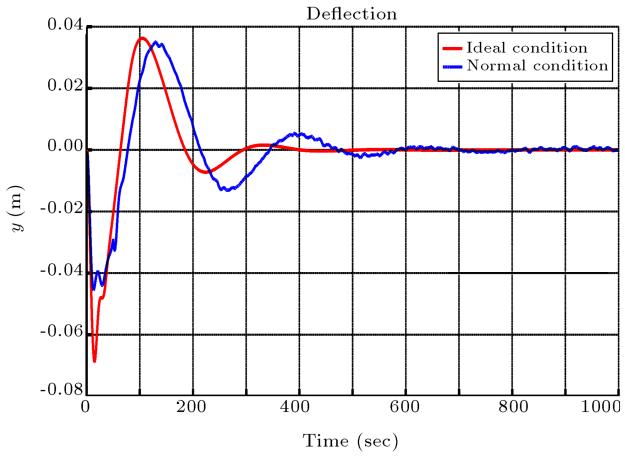

Figure 11d. Tip deflection, composite method.

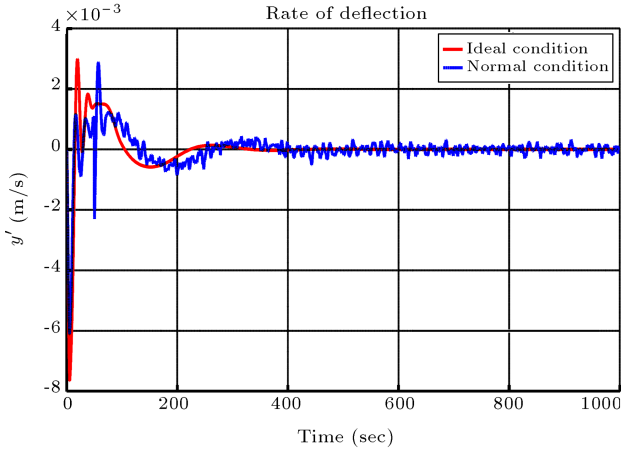

Figure 11e. Rate of tip deflection, composite method.

decreasing these weights the response performance improved whereas its robustness decreased.

Combined Controller

Figure 11 shows the simulation results of the composite controller. With the designed composite algorithm, the response of the pitch angle is shown in Figure 11a. We can see that the pitch angle approaches the reference trajectory at a time of 700s. Hence, fast and precise attitude control is achieved for the current design system. As compared to Figure 9a and Figure 10a (uncertain condition), in the dynamic inversion method, the response has a steady state error and cannot converge and, in the μ-synthesis method, the response has the largest overshoot and settling time.

Figure 11e shows the low frequency oscillation of the appendage in the composite method. The maximum tip deflection of the appendage in the dynamic inversion method is the largest and can be seen to be around 0.02 m (Figure 9e with uncertainty). Comparing rate of plots shown in Figures 11e and 9e, the composite controller has a larger rate of tip deflection caused by faster panel deflection damping.

The requirement for the momentum of each reaction wheel is illustrated in Figure 11c. As compared to Figures 9c and 10c, the composite method requires the largest controller effort.

A composite control algorithm has a larger controller order than the dynamic inversion method. In comparison with the μ-synthesis method, it has a smaller controller order (because the inner loop linear model is simpler and rigid). Overall, the composite control algorithm yields controllers which exhibit excellent performance and robustness for a broad range of operating conditions.

CONCLUSIONS

Vibration attenuation is a difficult control problem due to the stringent requirements on performance and the inherent characteristics of such structures. In this paper, flexible spacecraft pitch angle is controlled by three controller designs. The first controller is dynamic inversion, the second is μ-synthesis and the third is a composition of dynamic inversion and a μ-synthesis controller. It is assumed that only one reaction wheel is used. Actuator saturation is considered in the design of controllers.

Simulation results prove the composite controller ability in controlling attitude and, also, the suppression vibration of panels, which exhibit excellent performance and robustness for a broad range of operating conditions with minimal control effort.

It is interesting that these controllers damp the vibration of panels without considering damping terms and without using any filters.

In this paper, it is attempted to make sensor noise, disturbance and uncertainty close to real values. It is notable that this combined control method has never been used on spacecraft and seldom have all terms, such as disturbance, noise, uncertainty, non-linearity

and saturation, been considered in the simulations of flexible spacecraft.

REFERENCES

1. Tafazoli, S. and Khorasani, K. "Nonlinear control and stability analysis of spacecraft attitude recovery", *IEEE Transactions on Aerospace and Electronic Systems*, **42**(3), pp. 825-845 (2006).
2. Karkoub, M.A., Balas, G., Tamma, H. and Donath, M. "Robust control of flexible manipulators via μ-synthesis", *Control Engineering Practice*, **8**, pp. 25-734 (2000).
3. Zheng, J., Banks, S.P. and Alleyne, H. "Optimal attitude control for three-axis stabilized flexible spacecraft", *Acta Astronautica*, **56**, pp. 519-528 (2005).
4. Bang, H., Ha, C.K. and Kim, J.H. "Flexible spacecraft attitude maneuver by application of sliding mode control", *Acta Astronautica*, **57**, pp. 841-850 (2005).
5. Hu, Q. and Ma, G. "Variable structure control and active vibration suppression of flexible spacecraft during attitude maneuver", *Aerospace Science and Technology*, **9**, pp. 307-317 (2005).
6. Zhang, R. and Singh, S.N. "Adaptive output feedback control of spacecraft with flexible appendages", *IEEE Proceedings of the American Control Conference*, Arlington, VA, USA (25-27 June 2001).
7. Li, Z.B. Wang, Z.L. and Li, J.F. "A hybrid control scheme of adaptive and variable structure for flexible spacecraft", *Aerospace Science and Technology*, **8**, pp. 423-430 (2004).
8. Shahravi, M., Kabganian, M. and Alasti, A. "Adaptive robust attitude control of a flexible spacecraft", *International Journal of Robust and Nonlinear Control*, **16**, pp. 287-302 (2006).
9. Slotine, J.E. and Li, W., *Applied Nonlinear Control*, Prentice-Hall International (1991).
10. Kendi, T.A. and Doyle, F.J. "An anti-windup scheme for multi variable nonlinear systems", *Journal of Practice and Control*, **7**(5), pp. 329-343 (1997).
11. Bang, H., Tank, M.J. and Choi, H.D. "Large angle attitude control of spacecraft with actuator saturation", *Control Engineering Practice*, **11**, pp. 989-997 (2003).
12. Tandale, M.D., Subbarao, K. and Valasek, J. "Adaptive dynamic inversion control with actuator saturation constraints applied to tracking spacecraft maneuvers", *Journal of the Astronautical Sciences*, **52**(4), pp. 517-530 (2005).

BIOGRAPHIES

Heidar A. Talebi (M'02-SM'08) received his BS degree in electronics from Ferdowsi University of Mashhad in Iran, in 1988, his MS degree (with first-class honors) in electronics from Tarbiat Modarres University, Tehran, Iran, in 1991, and his PhD degree in electrical and computer engineering from Concordia University, Montreal, QC, Canada, in 1997. He was a Postdoctoral Fellow and a Research Fellow at Concordia University and the University of Western Ontario. In 1999, he joined Amirkabir University of Technology, Tehran, Iran, where he was the Head of the Control Systems Group from 2002 to 2004 and the Deputy Chair in research from 2008 to 2009. He is currently an Associate Professor and the Deputy Chair in education. His current research interests include control, robotics, fault diagnosis and recovery, intelligent systems, adaptive control, non-linear control, and real-time systems.

Maryam Malekzadeh received her BS degree (2002) in mechanical engineering from Sharif University of Technology, Tehran, Iran and her MS (2004) and PhD (2010) degrees in aerospace engineering from Amirkabir University of Technology, Tehran, Iran. Her main research interests are stability and control of non-linear systems, especially as applied to aerospace vehicles.

Abolghasem Naghash obtained his BS degree in mechanical engineering from Sharif University of Technology, Iran, in 1987. He, then, obtained his MS and PhD degrees in 1991 and 1995, respectively, in aerospace engineering, from the University of Minnesota. Since then, he has been a faculty member of the aerospace engineering department of Amirkabir University of Technology in Tehran, Iran. He is the author of several conference and journal papers in the area of aerospace vehicles, dynamics and control.